1990

# Analysis of Rigid Polyurethane Foams by Near-Infrared Diffuse Reflectance Spectroscopy

Charles E. Miller
*Haverford College*

Bruce E. Eichinger

# Analysis of Rigid Polyurethane Foams by Near-Infrared Diffuse Reflectance Spectroscopy

CHARLES E. MILLER and B. E. EICHINGER*
*Department of Chemistry, BG-10, University of Washington, Seattle, Washington 98195*

**The method of near-infrared diffuse reflectance spectroscopy is used to determine the compression and thermal properties of rigid polyurethane foams. Principal components analysis (PCA) of the spectra of the foams indicates that NIR spectroscopy can be used to discriminate between foams that were prepared from different polymeric formulations. Partial Least-Squares (PLS) calibrations of NIR spectra to the compression modulus, compression strength, deformation at failure, and K-factor (thermal conductivity) were also done. Results indicate that NIR spectroscopy can determine the compression modulus within 63.6 psi, compression strength within 2.63 psi, deformation at failure within 1.29%, and K-factor within 0.0089 Btu-in./°F-h-ft².**

Index Headings: **Analysis for polymer foams; Near-infrared spectroscopy; Reflectance spectroscopy.**

## INTRODUCTION

Rigid polyurethane foams are commonly used as insulation and packaging material.[1] The performance of a foam depends greatly on its compression and thermal properties. Physical testing methods, such as compression and thermal conductivity[2] tests, directly measure the physical properties of foams. However, these methods are usually destructive, are subject to high variability, and require substantial sampling times. In many situations, a faster, nondestructive analytical method is desired.

Near-infrared (NIR) diffuse reflectance spectroscopy has been used to rapidly and nondestructively sample materials that are similar to rigid foams with respect to optical properties.[3-6] NIR spectra contain absorption bands from overtones and combinations of fundamental molecular vibrations. As a result, this technology provides information about polymer composition and structure. Because the composition and structure of the polymer in a rigid foam greatly influences the physical properties of the foam, information from the NIR spectrum might be sufficient to provide good estimates of physical properties. In this work, the relationship between NIR spectra and several physical properties of rigid foams is investigated.

## EXPERIMENTAL

**Materials and Physical Measurements.** Polyurethane block copolymer foams were prepared from pure or polymeric 4,4'-diphenylmethane diisocyanate (MDI) and a variety of different polyols and chain-extenders. The diisocyanate and chain-extender provided the hard block of the polymers, and the polyol provided the soft block of the polymer. Samples for compression testing were prepared from one of, or a combination of, three different polyols: a PET-based polyester polyol, an aliphatic-based polyol, and an amine-based polyol. All of the foams contained small amounts of catalysts and surfactants.

A large (1 ft × 1 ft × ¾ in.) block of each polymer was formed, from which smaller blocks were cut for physical testing and NIR sampling. Two sample sets were obtained: (1) 26 samples were tested (see below) for compression properties (see Table I), and (2) 27 samples were tested for thermal conductivity (K-factor, see Table II).

Compression measurements (ASTM Method D1621-73)[7] were performed in triplicate, from three 2-in. × 2-in. blocks of each sample. A Universal Testing Machine (Instron, Canton, MA) was used for compression testing. Three 1-in. × 1-in. blocks, which were cut adjacent to the blocks used for compression testing, were used for NIR analysis. A stress/strain curve for a biaxial compression (perpendicular to the direction of elongation of voids in the foam) was obtained for each compression test sample. Three physical properties were obtained from this curve: (1) the compression modulus, (2) the compression strength, and (3) the percent deformation at failure. Samples that did not fail at 10% deformation were assigned a value of 10% deformation. For each property, the average of the three values obtained from triplicate tests was used for correlation to NIR spectra.

A K-matic heat flow meter (Holometrix, Cambridge, MA) was used to determine the K-factor of a 1-ft × 1-ft block of each sample (ASTM Method C518-85).[8] A smaller 2-in. × 2-in. block, which was cut adjacent to the sample used for the K-factor measurement, was used for NIR analysis.

In order to avoid errors caused by aging effects in the foams, NIR and physical testing methods were performed within several days of each other. The estimated error for each of the compression-measured properties was calculated as the pooled standard deviation of triplicate determinations of the property for all samples. The estimated error in the K-factor determination is obtained from Ref. 2.

**Spectroscopy.** NIR diffuse reflectance spectra were obtained with a Technicon InfraAlyzer 500/C grating instrument. The spectral range was 1100 to 2500 nm (in 2-nm increments), the nominal resolution was 10 nm, and the wavelength accuracy was 1 nm. Rigid foam blocks (1 in. × 1 in. × ¾ in., or 2 in. × 2 in. × ¾ in.) were placed on a sampling stage and covered with a quartz plate for NIR analysis. Each scan required approximately 2 min. Two replicate NIR scans for each block were obtained by sampling two opposite faces of the block.

Received 10 November 1989; revision received 18 December 1989.
* Author to whom correspondence should be sent.


0003-7028/90/4405-0887$2.00/0

TABLE I. Physical properties of compression-tested rigid foam samples.

| Sample number | Average values from compression test | | |
|---|---|---|---|
| | Modulus (psi) | Strength (psi) | Deformation (%) |
| 1 | 639 | 33.29 | 6.7 |
| 2 | 429 | 20.06 | 7.95 |
| 3 | 737 | 35.07 | 6.14 |
| 4 | 454 | 20.29 | 7.77 |
| 5 | 317 | 15.86 | 10 |
| 6 | 510 | 22.14 | 7.04 |
| 7 | 500 | 20.84 | 6.07 |
| 8 | 642 | 31.85 | 6.49 |
| 9 | 368 | 19.38 | 10 |
| 10 | 720 | 34.98 | 6.52 |
| 11 | 681 | 32.87 | 6.31 |
| 12 | 631 | 31.38 | 7.51 |
| 13 | 538 | 25.73 | 6.9 |
| 14 | 546 | 22.45 | 6.96 |
| 15 | 396 | 17.82 | 10 |
| 16 | 462 | 18.94 | 8.67 |
| 17 | 565 | 23.26 | 5.43 |
| 18 | 547 | 26.17 | 6.3 |
| 19 | 502 | 21.85 | 6.84 |
| 20 | 376 | 19.37 | 8.68 |
| 21 | 433 | 20.01 | 9.24 |
| 22 | 382 | 17.55 | 10 |
| 23 | 392 | 18.5 | 10 |
| 24 | 664 | 34.9 | 6.94 |
| 25 | 199 | 12.67 | 10 |
| 26 | 544 | 21.53 | 5.48 |

Correlation coefficients for intercorrelation of physical properties:

| | Modulus | Strength |
|---|---|---|
| Strength | 0.947 | 1 |
| Deformation | −0.802 | −0.664 |

TABLE II. K-factor-tested rigid foam samples.

| Sample number | K-factor (in Btu-in./°F-h-ft²) |
|---|---|
| 1 | 0.166 |
| 2 | 0.169 |
| 3 | 0.162 |
| 4 | 0.182 |
| 5 | 0.181 |
| 6 | 0.171 |
| 7 | 0.196 |
| 8 | 0.187 |
| 9 | 0.178 |
| 10 | 0.196 |
| 11 | 0.183 |
| 12 | 0.161 |
| 13 | 0.164 |
| 14 | 0.178 |
| 15 | 0.180 |
| 16 | 0.187 |
| 17 | 0.198 |
| 18 | 0.170 |
| 19 | 0.202 |
| 20 | 0.185 |
| 21 | 0.158 |
| 22 | 0.194 |
| 23 | 0.191 |
| 24 | 0.177 |
| 25 | 0.177 |
| 26 | 0.178 |
| 27 | 0.163 |

**Data Analysis.** Pre-analysis treatment of NIR spectra consisted of three steps: (1) averaging over samples, (2) averaging over wavelengths, and (3) correcting for scattering effects. For the K-factor-tested samples, duplicate spectra were averaged and adjacent wavelengths were averaged (resulting in 351 wavelength points for 27 spectra). For the compression-tested samples, three sets of duplicate spectra from the three blocks of each sample were averaged. Every other wavelength point, starting at 1102 nm, was removed, and every adjacent two wavelengths of those remaining were averaged (resulting in 176 wavelength points for 26 spectra). Multiplicative Scatter Correction (MSC)[9] was used to correct both sets of spectra for scattering effects after sample and wavelength averaging.

Principal Components Analysis (PCA)[10] of the spectra of the 26 compression-tested foam samples was performed with the Unscrambler software package (CAMO A/S, Trondheim, Norway). Partial Least-Squares (PLS)[4,11-13] calibration of NIR spectra to thermal and compression properties was also performed with the Unscrambler software package. For each PLS analysis, approximately half of the samples were used as a calibration set, and the remaining samples were used as a prediction set. The samples in the calibration set were used to construct a PLS calibration model that relates NIR absorbances to the physical property of interest. The samples in the prediction set were used to validate the PLS model. All PCA and PLS analyses use the mean-centered spectrum of each sample, which is determined as the spectrum of the sample minus the average of the spectra of the samples used in the analysis.

PLS calibration errors are expressed according to the Standard Error of Estimate (SEE) value

$$\mathrm{SEE} = \sqrt{\frac{\sum_{i=1}^{NC} (\hat{c}_{i,c} - c_i)^2}{(NC - 1)}} \qquad (1)$$

where $\hat{c}_{i,c}$ is the property of calibration sample $i$ that is estimated from the calibration model, $c_i$ is the known property of calibration sample $i$, and $NC$ is the number of calibration samples. The Standard Error of Prediction (SEP) is used to indicate prediction error:

$$\mathrm{SEP} = \sqrt{\frac{\sum_{i=1}^{NP} (\hat{c}_{i,p} - c_{i,p})^2}{(NP)}} \qquad (2)$$

where $\hat{c}_{i,p}$ is the property of prediction sample $i$ predicted from the calibration model, $c_{i,p}$ is the known property of prediction sample $i$, and $NP$ is the number of prediction samples.

The method of cross-validation[10,13] was used to determine the optimal number of factors for PCA and PLS analyses. The cross-validation procedure involves the removal of some of the samples in the calibration set, construction of a PCA or PLS model with the remaining samples, and subsequent prediction of the spectra (in the case of PCA) or physical properties (in the case of PLS) of the removed samples by the model. The optimal number of PCA or PLS factors is the number of factors at which prediction errors for the removed samples are minimized.

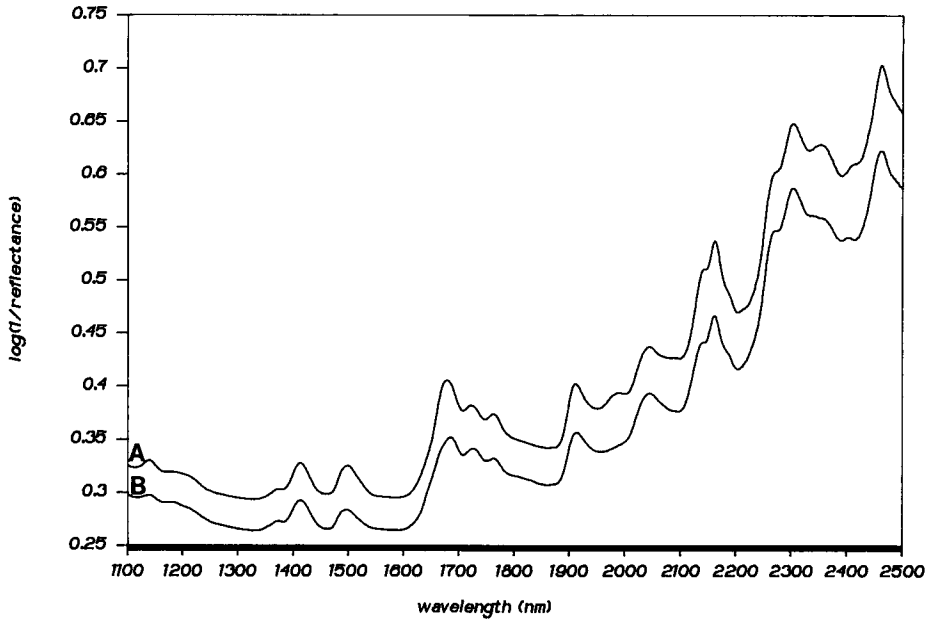


FIG. 1. Near-infrared diffuse reflectance spectra of compression-tested rigid foam sample 1 (**A**) and sample 2 (**B**).

## RESULTS AND DISCUSSION

**NIR Spectra of Rigid Foams.** The NIR diffuse reflectance spectra of two rigid polyurethane foams are shown in Fig. 1. These spectra have highly overlapped bands from CH, NH, and C=O groups in the samples. Bands in the regions 1100 to 1250 nm, 1600 to 1800 nm, and 2150 to 2500 nm are from aromatic and aliphatic CH groups. NH absorbances are found at approximately 1500 and 2050 nm, and C=O absorbances are in the region 1900 to 2100 nm. More specific assignments of NIR peaks can be made by reference to earlier NIR analyses of polymers.[14–16]

The differences in the two spectra in Fig. 1 originate from chemical and physical differences in the foam samples. The difference in baseline offset of the two spectra is a result of physical differences, or scattering differences, of the two samples. The differences in peak shape or relative peak amplitudes, such as those observed at approximately 1650–1750 nm, 1980–2050 nm, and 2250–2350 nm in Fig. 1, arise from differences in the chemistry of the samples. In this analysis, the MSC method[9] minimizes the scattering effects and leaves only the chemical effects to be used for calibration purposes.

**PCA of Compression-Tested Foams.** Cross-validation results indicate that three components of variation exist in the NIR spectra of the compression-tested foams. Table III shows the percentage of explained spectral variance for PCA models that have 1, 2, and 3 principal components. It should be noted that a significant amount of spectral variance (13.3%) is not explained by the three-principal component model. It is likely that this unexplained variance corresponds to the spectral noise level relative to the level of the spectral variance from chemical differences in the samples.

Figure 2, which shows a representative of the 26 samples in the space defined by the first two principal components, indicates the relationship between the spectra of the different foam samples. The most striking feature of this plot is the presence of four well-defined clusters of samples. Furthermore, it is known that each of these clusters corresponds to a specific polyol component in the polyurethane foams. Each cluster is assigned a cluster number of I to IV. Table III includes a list of the samples that belong to each cluster, as well as the polyol component that corresponds to each cluster.

In order to quantitate the degree of clustering observed in Fig. 2, several Euclidean distances in the three-dimensional PCA score space were calculated. For this

**TABLE III. Principal component analysis results for compression-tested foams.**

| Number of principal components in model | Percentage of spectral variance explained |
|---|---|
| Explained spectral variance: | |
| 1 | 52.6 |
| 2 | 73.1 |
| 3 | 86.7 |
| Observed sample clusters: | |
| Cluster I: 1, 3, 8, 10, 11, 12, 13, 18, 24 Aliphatic-based polyol | |
| Cluster II: 5, 9, 21, 23, 25 PET-based polyol | |
| Cluster III: 7, 15, 20, 26 PET-based and amine-based polyol | |
| Cluster IV: 2, 4, 6, 14, 16, 17, 19, 22 PET-based and aliphatic-based polyol | |

**TABLE IV. Distances in three-dimensional PCA score space.**

| | Cluster I | Cluster II | Cluster III |
|---|---|---|---|
| Distances between mean points of clusters: | | | |
| Cluster II | 0.543 | | |
| Cluster III | 0.496 | 0.541 | |
| Cluster IV | 0.469 | 0.560 | 0.423 |
| Average deviation of individual points from mean point of cluster: | | | |
| Cluster I: | 0.141 | | |
| Cluster II: | 0.141 | | |
| Cluster III: | 0.088 | | |
| Cluster IV: | 0.113 | | |

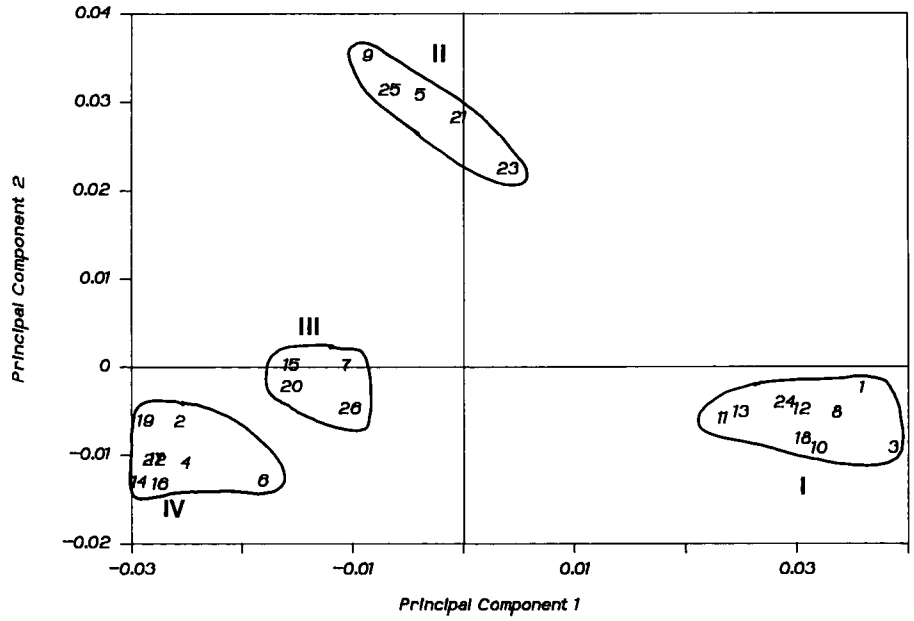


FIG. 2. Representative of the NIR spectra of compression-tested foam samples in the two-dimensional space defined by the first two principal component scores. Sample clusters are labeled I, II, III, and IV.

analysis, distances along each principal component axis were determined as the principal component score divided by the square root of the eigenvalue of that principal component. As a result, all three principal components have equal weight. Distances between the mean points of different clusters are compared to average deviations of individual points from their corresponding mean cluster point. Table IV shows the results of this analysis. All inter-cluster distances are much larger than the intra-cluster deviations. This result indicates that the clusters are well defined.

Trends in the PCA loading spectra indicate the identities of the polyol components corresponding to the different clusters. The loading spectra for the first and second principal components are shown in Figs. 3 and 4, respectively. Assignment of positive and negative bands in the loading spectra are aided by previous NIR analyses of poly(ether urethaneurea) copolymer,[14] poly(ethylene terephthalate) (PET),[15] and ethylene-propylene-diene terpolymer.[16] Positive peaks in the first principal component loading spectrum at 1142, 1674, 2142, and 2166 nm are aromatic CH bands of the MDI group. In addition, positive peaks are observed at 1910 and 1978 nm (from C=O groups) and at 1502 nm (from NH groups).

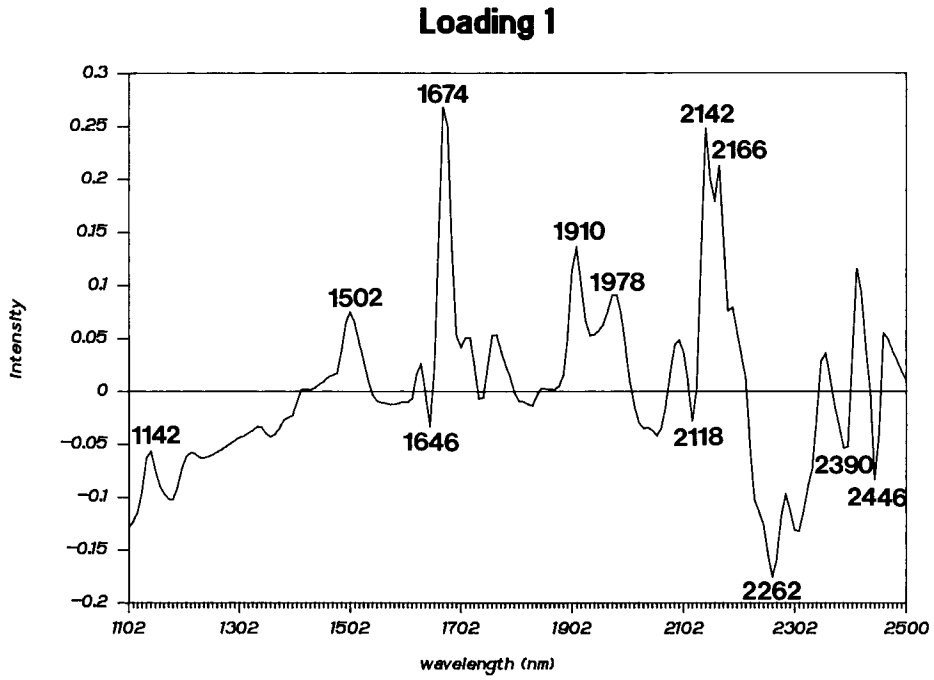


FIG. 3. First principal component loading spectrum, from principal components analysis of the NIR spectra of compression-tested foam samples.

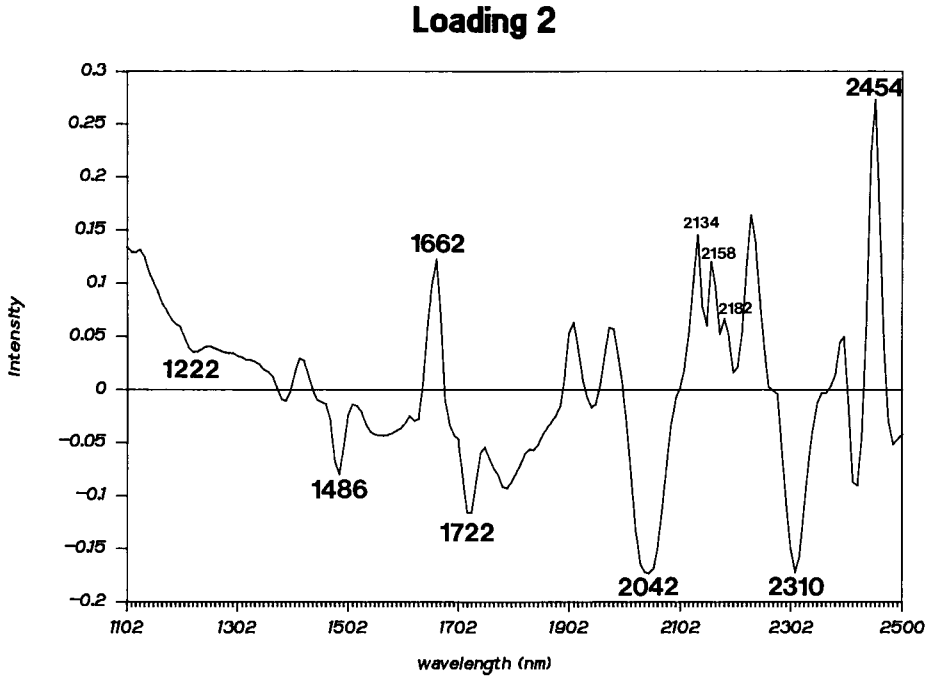


FIG. 4. Second principal component loading spectrum, from principal components analysis of the NIR spectra of compression-tested foam samples.

These results suggest that the first principal component is positively correlated to the fraction of MDI and urethane groups in the sample.

Negative peaks at 1646, 2118, and 2446 nm in the first principal component loading spectrum (Fig. 3) correspond to the aromatic CH vibrations of poly(ethylene terephthalate) (PET).[15] Other negative bands at 2262 and 2390 nm are from the ethylene groups in the ethylene glycol part of PET. These results indicate that the first principal component is negatively correlated to the fraction of PET-based polyol in the foams.

Positive bands in the second principal component loading spectrum (Fig. 4) at 1662, 2134, 2158, 2182, and 2454 nm are from aromatic CH groups in PET. Negative bands at 1486 and 2042 nm correspond to NH vibrations in the urethane groups of the polymers. Other negative bands at 1222, 1722, and 2310 nm are probably from ethylene groups in the polyol component of the polymer.

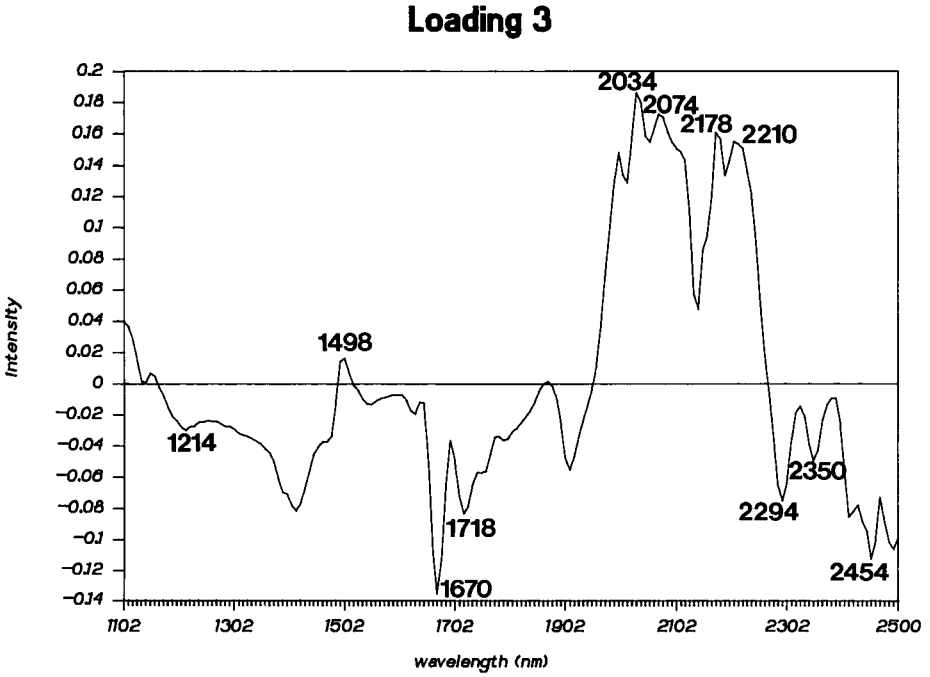


FIG. 5. Third principal component loading spectrum, from principal components analysis of the NIR spectra of compression-tested foam samples.

TABLE V. **Functional group correlations for three principal components of variation in NIR spectra of compression-tested foams.**

| Principal component | Functional groups in polymers | |
|---|---|---|
| | Positive correlation | Negative correlation |
| 1 | MDI, urethane | PET |
| 2 | PET | urethane, ethylene (aliphatic C-H) |
| 3 | MDI, urethane | PET, ethylene |

These results indicate that the second principal component is positively correlated to the amount of PET-based polyol in the polymers and negatively correlated to the amount of aliphatic-based polyol and urethane groups in the samples.

The third principal component explains a small, but significant, amount of variation in the spectra of the compression-tested foams. The third principal component loading spectrum, shown in Fig. 5, has positive peaks in the NH and C=O regions (1498, 2034, and 2074 nm) and negative bands in the ethylene CH regions (1214, 1718, 2294, and 2350 nm). The negative peaks at 1670 and 2454 nm probably correspond to aromatic CH vibrations in PET, and the positive peaks at 2178 and 2210 nm probably correspond to aromatic CH vibrations in the MDI group. These results indicate that the third principal component is positively correlated with the MDI and NH content of the polymers. Table V shows the summary of functional group correlations for the three principal components.

The PCA results indicate that the samples in cluster I, which have the highest values of the first principal component score and negative values of the second principal component score, must have the highest urethane content and lowest PET content. These results are consistent with the fact that the samples in cluster I contain an aliphatic-based polyol. Furthermore, the observation that these samples have the highest urethane content is consistent with the observation that they have the highest compression moduli[1] (consult Tables III and I).

The samples in clusters II, III, and IV have negative values of the first principal component score, which indicates that these samples each contain a PET-based polyol. The samples in cluster IV also have negative values of the principal component 2 score, which indicates that they also contain an aliphatic-based polyol. These results are consistent with the known correlations of polyol components to the different clusters of samples (Table III).

Figure 6 shows the representation of the foam samples in the space defined by principal components 1 and 3. The samples in clusters I, II, and IV have principal component 3 score values that are distributed about zero. However, all of the samples in cluster III have positive third principal component scores. If this result is combined with functional groups correlations of the third principal component (Fig. 5, Table V), it can be concluded that the samples in cluster III have significantly more NH content than the other samples. This result is consistent with the fact that these samples contain an amine-based polyol component, because an amine-based polyol would produce urea groups (each with two NH bonds) instead of urethane groups (each with one NH bond) upon reaction with isocyanate.

**PLS Calibrations for Compression Properties.** The results of PLS calibrations for compression modulus, compression strength, and percent deformation are shown in Table VI. The cross-validation results suggest that use of only two spectral factors for calibration to these properties. These results might appear contradictory to the PCA cross-validation results discussed earlier, which indicate that three sources of spectral variation are present. However, it is probable that the PLS cross-validation results are a better indicator of the optimal number of spectral factors for calibration to a specific property.

The calibration SEE values and prediction SEP values

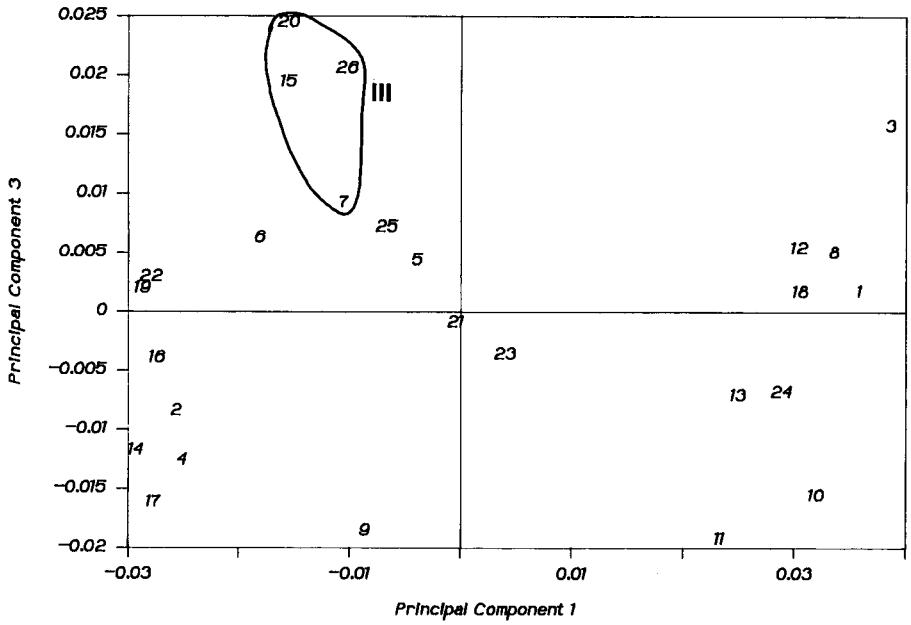


FIG. 6. Representation of the NIR spectra of compression-tested samples in the two-dimensional space defined by principal component 1 and 3 scores. Cluster III is identified.

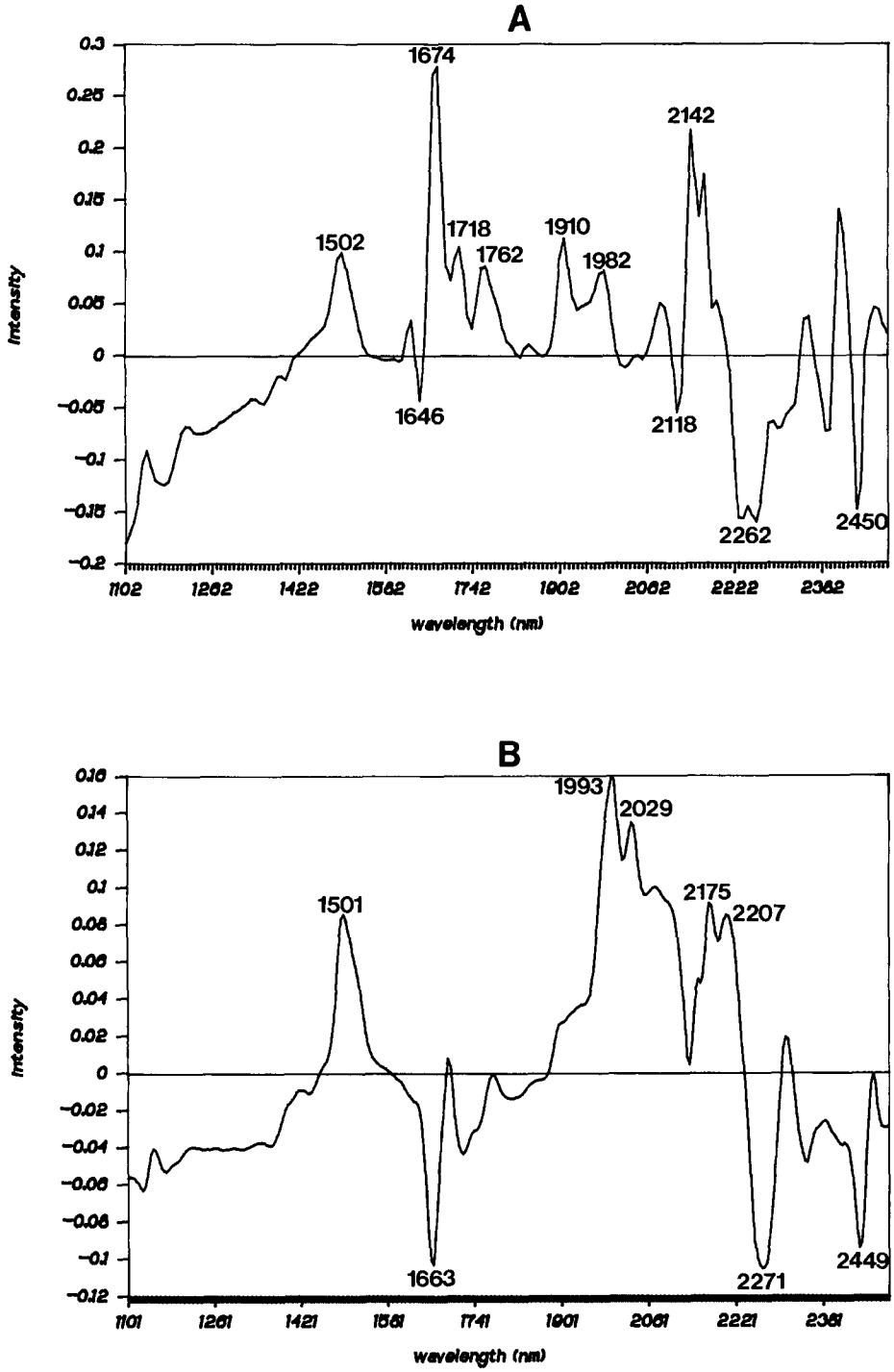


FIG. 7. First PLS loading spectra for the calibrations to compression modulus (A) and K-factor (B) of rigid polyurethane foams.

for the two-factor PLS calibrations are shown in Table VI. Estimated errors in the physical measurements of compression properties are also shown. These results indicate that NIR spectroscopy can predict compression modulus within 63.6 psi, compression strength within 2.63 psi, deformation at failure within 1.44%, and K-factor within 0.0089 Btu-in./°F-h-ft$^2$. The modulus and strength calibrations are the most accurate, in terms of relative calibration and prediction error. However, the standard error of calibration and prediction for each property is only slightly greater than, or less than, the estimated error in the physical measurement. This result suggests that errors in the physical measurements are the major source of calibration and prediction errors.

The first PLS loading spectrum for the compression modulus calibration, shown in Fig. 7A, indicates the NIR spectral features that are positively and negatively correlated to the compression modulus of the foams. Positive features at 1674 and 2142 nm are from aromatic CH vibrations in the MDI group. The positive band at 1502 nm corresponds to the urethane NH group, and the positive bands at 1910 nm and 1982 nm correspond to the

TABLE VI. Results of PLS correlations of physical properties to NIR spectra of rigid polyurethane foams.

| Physical property (units) | Error of physical measurement | SEE | Relative calibration error (%) | SEP | Relative prediction error (%) | Number of PLS factors used[a] |
|---|---|---|---|---|---|---|
| Compression modulus (psi) | 50.3[b] | 53.2 | 9.89 | 63.6 | 20.3 | 2 |
| Compression strength (psi) | 1.84[b] | 1.95 | 8.71 | 2.63 | 17.2 | 2 |
| Deformation at failure (%) | 1.29[b] | 0.88 | 19.3 | 1.44 | 39.0 | 2 |
| K-factor (Btu-in./°F-h-ft²) | 0.013[c] | 0.0095 | 21.6 | 0.0089 | 26.2 | 2 |

[a] The optimal number of PLS factors is determined by cross-validation.
[b] Determined as pooled standard deviation of triplicate measurements.
[c] Obtained from Ref. 2.

urethane carbonyl group. These results indicate that modulus increases with increasing fraction of urethane and MDI groups in the foam. Positive ethylene bands at 1718 and 1762 nm indicate a positive correlation between modulus and ethylene content. The negative features are dominated by PET bands (1646, 2118, 2262, and 2450 nm). The positive ethylene bands and negative PET bands indicate that, for a given fraction of MDI groups in the polymer, the foams with the aliphatic polyol component have a higher modulus than the foams with the PET-based polyol components. Because the three compression properties are highly intercorrelated (see Table I), first PLS loading spectra for strength and deformation have very similar features. The functional group correlations for strength are the same as those for compression modulus, and the correlations for deformation are exactly opposite to those for compression modulus.

**PLS Calibration for K-factor.** The results for the PLS calibration to K-factor are shown in Table VI. Cross-validation results indicate that two spectral factors are necessary for the calibration. Although the SEE and SEP values are large relative to the range of values used in the calibration, the absolute SEE and SEP values are lower than the estimated error of the physical K-factor measurement (0.013).[2] As a result, the errors in the physical measurements are probably the main contributor to the calibration and prediction errors.

The first PLS loading spectrum for the calibration to K-factor is shown in Fig. 7B. Positive bands at 1501, 1993, and 2029 nm correspond to NH and carbonyl absorbances. The negative peaks at 1663 and 2449 nm correspond to the aromatic CH groups in PET, and the negative peak at 2271 nm corresponds to the ethylene glycol group in PET. These results indicate that the thermal conductivity of the foams is positively correlated to the fraction of urethane groups and negatively correlated to the PET content of these foams.

## CONCLUSION

This study demonstrates that NIR diffuse reflectance spectroscopy can be used to rapidly and nondestructively determine physical properties of rigid polyurethane foams. The chemical information provided by NIR spectroscopy enabled accurate determinations of compression and thermal properties. Although NIR spectroscopy is not expected to provide information about other factors that influence physical properties, such as void density and size, and levels of trace constituents in the foams, it can be used to make acceptable predictions of physical properties.

It is important to note that the formulation (or polyol component) was the major source of variation of the foam samples used in this work. As a result, the studies in this work primarily indicate the effect of formulation on the spectra and properties of rigid foams. An additional study that uses foams of the same formulation, but with different compositions (or relative percentage of MDI and polyol) could be used to determine the effects of composition and other factors on the NIR spectra and physical properties or rigid foams.

## ACKNOWLEDGMENTS

The authors wish to thank ICI Polyurethanes for generous support of this work. Specific acknowledgments go to W. W. Brand, for coordination of this research effort with ICI, and A. J. Flint, for the acquisition of samples and information regarding physical testing of samples. Physical tests performed by W. L. Finerty are gratefully acknowledged.

1. K. C. Frisch and S. L. Reegen, *Advances in Urethane Science and Technology* (Technomic, Stamford, Connecticut, 1971).
2. S. A. Smith, C. J. Galbraith, M. J. Cartmell, M. L. Moore, and R. K. Brown, Paper delivered at the Polyurethanes World Congress (1987), p. 74.
3. E. Stark, K. Luchter, and M. Margoshes, Appl. Spectrosc. Rev. **22,** 335 (1986).
4. P. Williams and K. Norris, *Near-infrared Technology in the Agricultural and Food Industries* (American Association of Cereal Chemists, St. Paul, Minnesota, 1987).
5. L. G. Weyer, Appl. Spectrosc. Rev. **21,** 1 (1985).
6. C. E. Miller and T.-K. Yin, J Mat. Sci. Lett. **8,** 467 (1989).
7. *1989 Annual Book of ASTM Standards,* ASTM Method D1621-73 (ASTM, Philadelphia, 1989), Vol. 08.02, p. 11.
8. *1988 Annual Book of ASTM Standards,* ASTM Method C518-85, (ASTM, Philadelphia, 1988), Vol. 04.06, p. 151.
9. P. Geladi, D. MacDougall, and H. Martens, Appl. Spectrosc. **39,** 491, (1985).
10. I. T. Joliffe, *Principal Components Analysis* (Springer-Verlag, New York, 1986).
11. K. Beebe and B. R. Kowalski, Anal. Chem. **59,** 1007A (1987).
12. P. Geladi and B. R. Kowalski, Anal. Chim. Acta **185,** 1 (1986).
13. D. M. Haaland and E. V. Thomas, Anal. Chem. **60,** 1202 (1988).
14. C. E. Miller, P. G. Edelman, B. D. Ratner, Appl. Spectrosc. **44,** 576 (1990).
15. C. E. Miller and B. E. Eichinger, Appl. Spectrosc., **44,** 496 (1990).
16. C. E. Miller, Appl. Spectrosc. **43,** 1435 (1989).